SUT
Society for Underwater Technology

PROCEEDINGS

9th International SUT Offshore Site Investigation and Geotechnics Conference

Innovative Geotechnologies for Energy Transition

12-14 September 2023 | London, UK

www.sut.org | www.osig2023.com

Offshore Site Investigation and Geotechnics

Innovative Geotechnologies for Energy Transition

Proceedings of the 9th International Conference
12-14th September 2023

Imperial College, London, UK

Jointly sponsored by:

Fugro
Ocean Infinity
Seaway7
NextGeo
Bluefield Geoservices
bp
XOCEAN
Alpine
RINA
Ternan Energy
GDS Instruments
Gavin & Doherty Geosolutions (GDG)
Wood Thilsted
NGI
RWE
Atkins
Geowynd
ERM MarineSpace
Inosys
Vysus

SUT
Society for Underwater Technology

Organised by the Offshore Site Investigation and Geotechnics Committee of the Society for Underwater Technology

Published by the Society for Underwater Technology

Offshore Site Investigation and Geotechnics ISSN 2754-6322 (Online)

ISBN 0 906940 59 1
ISBN 978-0-906940-59-4

A CIP Catalogue record for this book is available from the British Library.
First published in 2023 by
The Society for Underwater Technology
Nunn Hayward LLP, 2-4 Packhorse Road, Gerrards Cross, SL9 7QEN

Session 18 – Suction Installed Foundations

Session 19 - Foundation Performance and Ground Characterisation

Load-time failure envelopes for suction caissons under sustained vertical loading

A. Rosati & A. Desideri & S. Rampello
Department of Structural and Geotechnical Engineering, Sapienza University of Rome, Rome, Italy
M.F. Randolph & C. Gaudin
Centre for Offshore Foundation Systems, Oceans Graduate School, the University of Western Australia, Perth, Australia

ABSTRACT: Suction caissons are established as a reliable anchoring system to moor a range of offshore floating facilities. Under sustained loads, generally characterized by long durations, the caisson holding capacity against uplift loading, that relies on suction pressures induced within and at the base of the soil plug, is expected to reduce over time, due to the equalization of pore water pressures. The scarcity of studies addressing this sustained loading problem has motivated this study, in which the response of suction caissons in soft clay subjected to sustained vertical uplift loads is investigated through finite element simulations and centrifuge model tests. Results are presented in the form of failure envelopes in the load-time plane, correlating, for each failure mechanism detected, the load level to the corresponding holding time. The findings of this study are considered useful for concept design purposes, when sustained loads govern the caisson design.

1 Introduction

Suction caissons are cylindrical thin-walled units with an open bottom and a closed top equipped with a valve. They are established as a reliable anchoring system to moor a range of offshore floating facilities in medium to ultra-deep waters. They benefit from relatively low cost, ease of installation and decommissioning, as well as lower impact on marine wildlife, compared to alternative systems.

For medium to deep water installations, suction caissons are characterized by diameters in the range 3−10 meters and length to diameter ratios in the range 3-8 (Randolph and Gourvenec, 2011). Smaller ratios are also possible for floating facilities in shallower water.

The installation process of a suction caisson consists generally of two phases: (i) the anchor penetrates under self-weight with free evacuation of the water located inside the skirts with the valve in the caisson lid open; (ii) an additional driving force is created by pumping out the water trapped between the caisson lid and the top of the soil plug with the valve closed. The valve remains closed after reaching the required embedment.

In this context the term *suction* (p_{int}-$p_{out} < 0$) represents the value of water pressure inside the caisson (p_{int}) net of the hydrostatic pressure acting outside the caisson (p_{out}), which results from two different aspects characterizing this foundation system: (i) the active (i.e. controlled) reduction of water pressure inside the caisson during the installation process and (ii) the passive reduction of pressure mobilized during uplift, which represents one of the main resisting forces for the anchor.

Suction anchors can be subjected to a combination of loadings, vertical or inclined, according to the mooring system adopted, that can be distinguished by permanent (e.g. mooring line pretension loads), quasi-static (e.g. mean wind, mean current, tides), and cyclic (e.g. hurricane, storm loads) components.

As far as vertical loads are concerned, there are several studies, both of a physical and numerical nature, focusing on the assessment of the monotonic uplift capacity of the soil-foundation system. These provide simplified prediction procedures of such capacity (Andersen and Jostad, 2002, 2004; Deng and Carter, 2002; Jeanjean et al., 2006; Chen et al., 2009; Gourvenec and Clukey, 2018).

It is well established that, depending on the loading rate and whether free flow of water is possible through the top cap of the caisson, three uplift resisting mechanisms are possible: (i) reverse end bearing; (ii) caisson pull-out; (iii) plug failure. Mechanism (i) can be relied upon only if the caisson top cap is sealed (no free flow of water) and the loading rate is sufficiently high to force an undrained response of the soil. Mechanism (ii), on the other hand, can be triggered if the top cap is unsealed, as for caisson retrieval during decommissioning, or if the loading rate is low enough to allow for a fully drained response of the soil and the development of a sliding failure along the internal and external walls of the caisson. Finally, mechanism (iii) can be regarded as an intermediate case in which the soil response is partially drained and the

developed passive suctions hold the soil plug within the caisson as it is pulled from the ground, until a tensile failure is reached at the tip level. Net of the caisson weight, the force components contributing to the holding capacity differ according to the failure mode: external friction + reverse end bearing, the latter mobilised thanks to the passive suctions developed during uplift, in (i); external + internal friction in (ii); external friction + submerged weight of the plug in (iii).

While in the case of cyclic loads, generally characterized by high frequencies, the design assumption is that the soil response is undrained, in the case of quasi-static loads on a sealed caisson attention must be paid to the change of drainage conditions that occur over time. Indeed, quasi-static loads, also known as sustained loads, despite their oscillatory nature, differ from the cyclic loads for having higher periods and generally long durations of weeks or even months. Under such conditions the caisson capacity to withstand uplift loads, relying on suction pressures induced at the base and within the soil plug, becomes questionable, due to the progressive equalization of pore water pressures (p.w.p.) over time. Specifically, due to the difference of p.w.p. in the soil outside from that inside the caisson, water starts to flow from the outside towards the inside of the caisson causing the soil to swell. This produces a progressive reduction of effective stresses within the plug and, in turn, of the internal friction. Consequently, a reduction of the holding capacity from the reverse end bearing value to that associated with one of the mechanisms of caisson pull-out or plug failure may occur over time. Because of this, as reported in Clukey et al. (2004) for some deep-water facilities in the Gulf of Mexico subjected to loop current events, there are practical cases in which sustained loads control the suction caissons design, despite their value being lower than that associated with hurricane loads.

A few studies are available in the scientific literature on the topic of suction anchors in clay subjected to sustained loads, including the works from Clukey and Phillips (2002) and Randolph and House (2002), based on centrifuge tests, and Al Khafaji et al. (2003), based on finite element (FE) simulations. Results from these are compared in Clukey et al. (2004).

The above studies, however, address a very specific design problem, concerning specific combinations of anchor geometry and soil parameters, and do not deal with the topic in a systematic way, so as to provide a basis to a general procedure for assessing the safety of soil-anchor systems under sustained loading. More recent is the study by Chen and Randolph (2007), where the results of centrifuge tests, conducted on suction caissons in different clayey soil types, are used to determine *corrected* capacity factors to be used in conventional design procedures, to indirectly account for the effects of the soil drainage response.

In this study, results of numerical and physical modelling tests are used to investigate the failure mechanism to be expected and the corresponding limit holding time as a function of the applied sustained load level, as well as to establish a relationship of general validity defining the evolution of the uplift capacity over time.

2 Finite element modelling

For this study axisymmetric small strain FE simulations, based on coupled pore fluid diffusion/stress analyses, were performed using Abaqus/Standard.

2.1 *Numerical model*

The model included a rigid caisson, wished-in-place, and a homogeneous layer of normally consolidated clay, whose non-linear behavior was described using the Modified CamClay (MCC) model (Roscoe and Burland, 1968). The physical, mechanical, and hydraulic parameters of the clay, adopted in the FE simulations, are listed in Table 1.

Table 1. Soil parameters adopted in the FE simulations

Parameter	Value
effective unit weight, γ' (kN/m^3)	6.81
coefficient of earth pressure at rest, k_0	0.65
initial void ratio, e_0	1.5
Poisson's coefficient, ν	0.3
swelling index, κ	0.041
swelling over compression index, κ/λ	0.163
inclination of critical state line, M	0.8
permeability, k (m/s)	4e-9

The caisson, characterized by an external diameter D=3.6 m, length over diameter ratio L/D=3, and a wall thickness t=0.1 m, was discretized by means of 4-node bi-linear stress/displacement elements with reduced integration (CAX4R), while 4-node bilinear displacement and pore pressure elements with reduced integration (CAX4RP) were used for the discretization of the soil domain. The FE mesh used in the study is shown in Figure 1. The model dimensions, equal to 8 D/2 and 3 L, respectively along the radial and vertical axis, were chosen so that the boundaries were far enough so as to not influence the simulation results in terms of displacement, strain and stress fields.

The radial component of the displacements was restricted along both the symmetry axis and the outer radial perimeter of the domain, while radial and vertical components of displacement were restricted at the bottom of the domain. An initial hydrostatic p.w.p. distribution was assumed, starting from zero at the seabed. A fixed p.w.p. of p = 0 kPa was prescribed at the seabed outside the caisson and a hydrostatic pressure of p (z) = $\gamma_w z$, with z being the nodal depth in the mesh, was fixed at the outer radial boundary and at the bottom of the FE model in order to allow

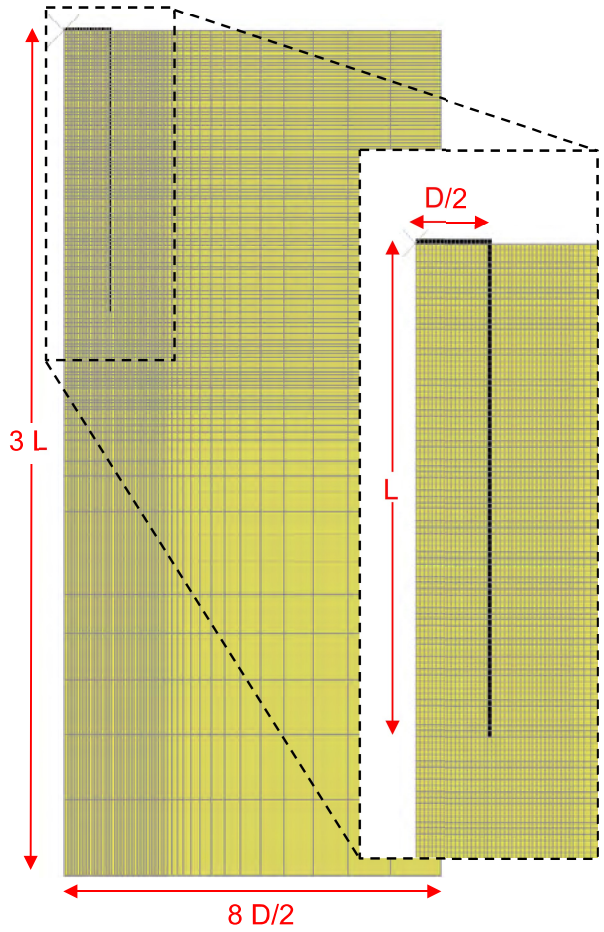

Figure 1. FE mesh used in this study

water to flow freely into the domain. The axis of symmetry was set as an impermeable boundary.

The interaction between the caisson and the surrounding soil was modelled by means of the contact pair algorithm based on a slave-master surface-to-surface approach. The following assumptions were made: (a) surface separation was allowed at the skirt tip contact and at the lid-plug contact, the latter only during the simulations of the caisson pull-out mechanism, as detailed in the following; (b) no separation was allowed along the internal and external skirt contact; (c) the tangential behavior was described by means of the Coulomb friction model, i.e. a rigid-perfectly plastic model, in which the maximum value of shear stress is computed as $\tau_{lim} = \mu \sigma'_n$, μ being the friction coefficient and σ'_n the effective normal stress. A value of $\mu = 0.2$, being in the range of those experimentally determined by Chen and Randolph (2007), was adopted. A smooth interface was adopted at the lid-plug contact only.

For simplicity, and to isolate the effect of sustained loading, the numerical simulations ignored the installation process, as well as the loading of the soil due to the self-weight of the caisson. The same approach was used in the centrifuge tests, whereby the measure of the caisson self-weight was zeroed from the load cell prior to the installation, as described in the next section. Such a choice is justified by the fact that the reaction forces, exchanged between the caisson and the surrounding soil during uplift, such as suction, external and internal friction, depend on the net uplift force applied to the caisson; hence they are independent of the caisson self-weight. The caisson self-weight clearly contributes to the overall capacity of the caisson, but, in view of the above, in this study all results are presented net of this component.

The numerical simulations addressed the assessment of (i) the maximum uplift capacity expressed by the system when it is rapidly loaded and the soil response is fully undrained, (ii) the minimum uplift capacity expressed by the system when it is slowly loaded and the soil response is fully drained, (iii) the response over time of the caisson under a sustained load, equal to a fraction of the undrained capacity, as a consequence of the change in the soil drainage conditions. Analyses (i) and (ii) determined the holding capacity associated with the mechanisms of reverse end bearing, V_u^{rev}, and caisson pull-out, V_u^{caiss}.

After the initial equilibrium configuration was established under the soil self-weight, a displacement-controlled and a load-controlled approach were employed in (i-ii) and (iii), respectively. In particular, in (i-ii) a single additional calculation phase was performed, in which the caisson was pulled out at a constant rate until failure conditions were attained, with failure indicated by a lack of convergence in the FE code. By contrast, in (iii) two additional calculation phases were performed, in which first a prescribed uplift load was applied rapidly to the caisson, and subsequently the load was held constant until a failure condition was attained.

In (i) the pull-out velocity was chosen high enough to ensure that a higher velocity did not result in a higher calculated capacity, given that the soil model is rate-independent. In this way, a perfectly undrained response in the soil, characterized by no volumetric strains, was ensured, in agreement with Deng and Carter (2002). In (ii) a permeability value of 1 m/s was assigned to force a drained response of the soil.

Finally, differently from (i) and (iii), in (ii) suction pressures within the plug were prevented by allowing separation between the under-lid and the top of the soil plug surfaces, the latter being treated as a drainage boundary by imposing a prescribed boundary condition of $p = 0$ kPa, similarly to the remaining nodes on the seabed outside the caisson.

2.2 *Results from numerical modelling*

First of all, the values of $V_u^{rev} = 1927$ kN and $V_u^{caiss} = 957$ kN ($V_u^{caiss}/ V_u^{rev} = 0.5$) were determined by means of the displacement-controlled analyses (i-ii) described in the previous section. Subsequently, the value of uplift capacity associated with the mechanism of plug failure was obtained by adding the value of the external friction, numerically computed in the caisson pull-out simulation, to the value of the submerged weight of the soil plug, thus obtaining $V_u^{plug} = 1233$ kN ($V_u^{plug}/ V_u^{rev} = 0.64$).

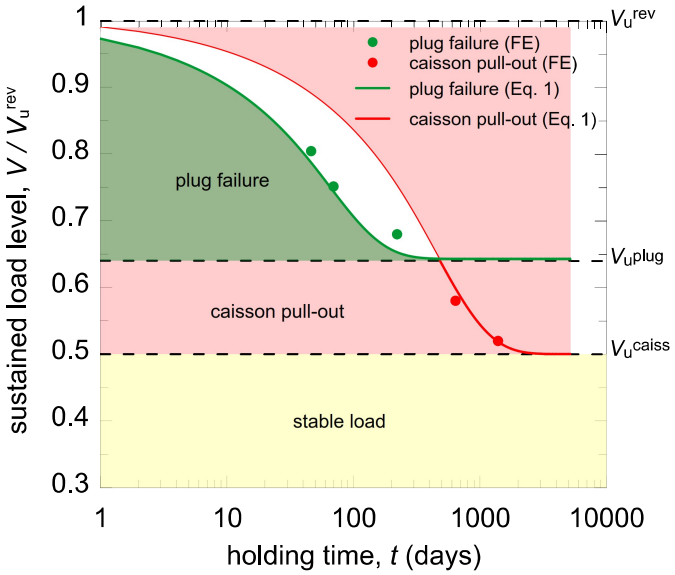

Figure 2. Results of the FE simulations (dots) and analytical curves (Eq. 1)

Five sustained loading simulations (iii in the previous section) were then performed, each of them imposing a different value of sustained load level higher than V_u^{caiss}/ V_u^{rev} (V/ V_u^{rev} = 0.8, 0.75, 0.68, 0.58, 0.52). The results of such simulations are represented by the dots in the sustained load-holding time plane shown in Figure 2. The values of the uplift capacity associated with the three mechanisms of reverse end bearing, plug failure and caisson pull-out are also represented and highlighted by the dotted lines. Each dot in Figure 2 represents the combination of the sustained load applied and the limit holding time, corresponding to the attainment of a failure condition of the soil-anchor system, as obtained from the numerical simulation. In green are represented the results of the numerical simulations resulting in a plug failure, whereas those in red resulting in a caisson pull-out by frictional failure along the internal and external shaft. The former were characterized by diffused tensile vertical effective stresses at the base of the plug long before the frictional capacity at the soil-internal shaft contact was fully mobilized. On the other hand, the latter were characterized by the full mobilization of such frictional capacity while no tensile stresses were reached in the soil domain.

The difference between the mechanism detected for higher load levels (plug failure) and for lower load levels (caisson pull-out) is associated with the different flow paths of the water through the soil, as well as different values of the hydraulic gradient generated by the passive suctions induced by the rapid application of the load. For higher loads, indeed, the value of the passive suction mobilized under the lid is higher, thus resulting in a higher value of the hydraulic gradient between the soil outside and inside the caisson. Consequently, more significant flow of water is induced, as is evident by the order of magnitude difference in the scale of values in Figure 3 and 4, where the vector plot of the pore water unit flux at failure is represented for sustained loads of V = 1448 kN (i) and 1002 kN (ii), for which initial suctions of -93 and -48 kPa were computed, respectively.

Moreover, from the comparison of Figure 3 and 4, it is also possible to observe the different flow paths in the two cases: in (i) the flow is concentrated in the soil in the immediate proximity of the caisson tip and in the lower part of the plug, whereas in (ii) the water flows through the base and whole plug up to the top. The heavy flow of water towards the base of the plug causes in (i) concentrated swelling of the soil at the tip level, consistent with the observed strong reduction of effective stresses that lead to tensile failure of the plug. By contrast, in (ii) the water flowing through the whole plug allows for diffused swelling of the soil, resulting in progressive mobilization of the internal friction along the plug-caisson contact, starting from tip level.

In order to highlight this aspect, plots of the mobilized shear stresses and the caisson-plug relative displacement computed at failure along the internal contact are also shown in Figure 3 and 4. For the sake of clarity cyan arrows are added to locate the position at which the transition from a *stick* to a *slip* condition is observed along the internal contact. It may be seen that tensile (plug) failure in Figure 3 is triggered long before full mobilization of the internal friction, whereas in Figure 4 the internal friction is fully mobilized. Finally, the shorter flow path lengths in (i) compared with in (ii) justifies the very different limit holding times observed, equal to 69 days in (i) and 1377 days in (ii).

The numerical results presented in Figure 2 are interpreted by a set of two curves (green and red lines) describing the evolution of the resisting forces, $R^{plug}(t)$ and $R^{caiss}(t)$, associated with the mechanisms of plug failure and caisson pull-out, respectively, over time. The equations of the curves are given by

$$R^{plug}(t) = V_u^{rev} - \left(V_u^{rev} - V_u^{plug}\right)\bar{U}_{hor}(t)$$
$$R^{caiss}(t) = V_u^{rev} - \left(V_u^{rev} - V_u^{caiss}\right)\bar{U}_{ver}(t) \quad (1)$$

where V_u^{rev}, V_u^{plug} and V_u^{caiss} (kN) are the monotonic uplift capacity of the soil-anchor system associated with the mechanisms of reverse end bearing, plug failure and caisson pull-out, respectively, and $\bar{U}_{hor/ver}(t)$ is the average degree of consolidation calculated according to Terzaghi's one-dimensional consolidation theory. The value of U is a function of time, soil consolidation coefficient and consolidation path length, assuming a rectangular isochrone.

Based on the observations just presented, the objective of Equation 1 is to describe the complex evolution of the uplift capacity of the system, associated with a clearly two-dimensional swelling process of the soil, by means of a simple analytical tool in which the average degree of consolidation, $\bar{U}_{hor/ver}(t)$, is a measure of the progress of the process over time. The tool is based on the simplifying assumption that the plug failure and the caisson pull-out mechanisms are

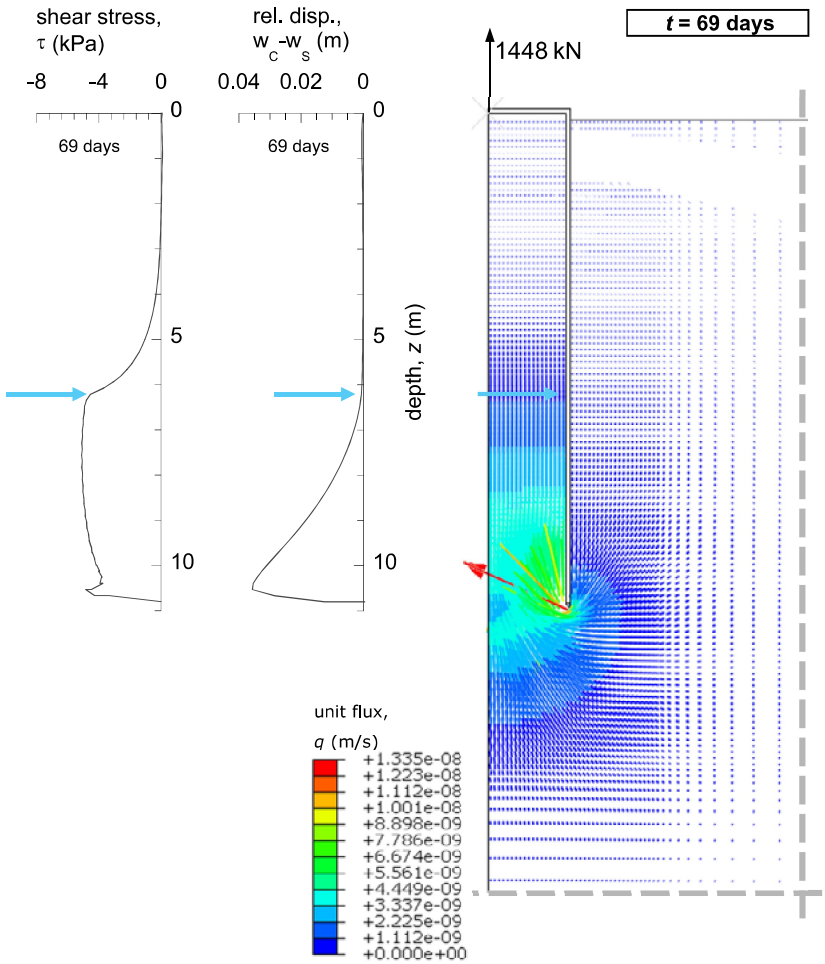

Figure 3. Vector plot of pore water unit flux at failure under a sustained load of V = 1448 kN

associated with a one dimensional, mainly horizontal, and vertical, respectively, swelling process along path lengths, defined as s_{hor} (m) and s_{ver} (m), respectively, both of which are a function of the anchor geometry.

In particular, based on the results of a parametric study, where the soil-anchor system mechanical and geometric parameters have been varied (not presented here since outside the paper length limit), lengths of $s_{hor} = 1.5D$ and s_{ver} given by a function of L (m) and L/D, were adopted for computation of $\overline{U}_{hor}(t)$ and $\overline{U}_{ver}(t)$, respectively. The value of s_{ver} is given by

$$s_{ver} = L\left[\pi - \tan^{-1}\left[5\left(\frac{L}{D}\right)^{0.85}\right]\left(2 - \frac{2}{\pi}\right)\right] \quad (2)$$

based on that proposed by Senders and Randolph (2009) for the seepage length for steady state flow of water from outside the caisson and up the soil plug for suction caisson installation in sand. Such steady state conditions develop near the onset of caisson pull-out, as shown by Mana et al. (2014).

Moreover, to account for the different depths of the soil volumes associated with the two swelling processes, the value of the swelling coefficient is calculated at reference depths of $z^{ref}_{hor} = L + D/2$ and $z^{ref}_{ver} = L - D/2$, for the computation of $\overline{U}_{hor}(t)$ and $\overline{U}_{ver}(t)$, respectively. It is important to emphasise that, in the computation of $\overline{U}_{hor/ver}(t)$, a *swelling* coefficient rather than a *consolidation* coefficient is used, given as a function of the soil hydraulic and mechanical parameters by

$$C_{swell} = \frac{k}{\gamma_w}\frac{1+e_0}{\kappa}\sigma'_v(z^{ref}) \quad (3)$$

where γ_w (kN/m^3) is the water unit weight, $\sigma'_v(z^{ref})$ (kPa) is the vertical effective stress computed at a depth equal to z^{ref} (m) and the remaining parameters are defined in Table 1. Such an assumption is justified by the extensive, rather than compressive, stress paths that the soil inside and at the base of the caisson undergoes over time.

Despite the simplified assumptions underlying the analytical tool, Figure 2 shows that the curves are able to satisfactorily interpret the numerical results for both mechanisms. Such an observation would justify the use of the curves as a predictive tool at a concept design stage to evaluate the behaviour of the soil-anchor system under sustained vertical loads in load-time space. Indeed, the minimum envelope obtained by the set of two curves defines a failure envelope enclosing, on its left side, all the safe combinations of sustained load level and holding time, with the additional advantage to be able to predict the failure mechanism as a function of the sustained load level applied. For clarity the shaded areas in Figure 2 are represented to highlight the portions of load-time space where a plug failure (green) and a caisson pull-out (red) is expected, whereas for $V < V_u^{caiss}$ (yellow) the caisson is expected to remain stable over time.

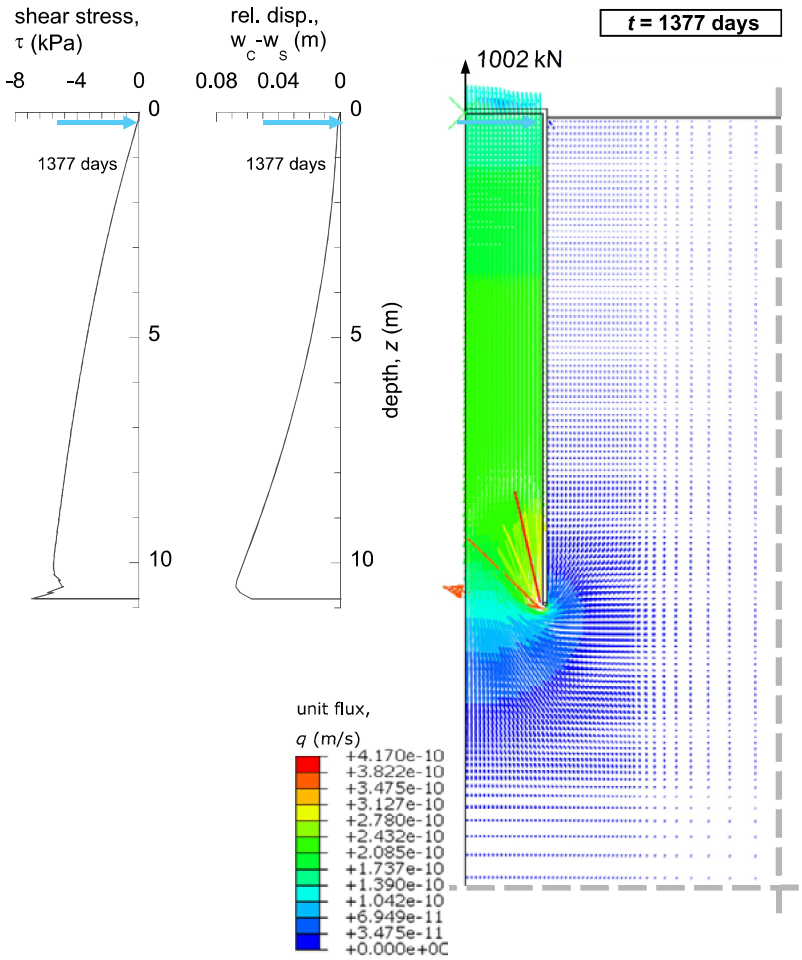

Figure 4. Vector plot of pore water unit flux at failure under a sustained load of $V = 1002$ kN

3 Physical modelling in the centrifuge

Five centrifuge tests (T01-T05) were conducted in a soil sample consisting of normally consolidated kaolin clay using the 5 m-radius C72 beam centrifuge of the National Geotechnical Centrifuge Facility (NGCF) at the University of Western Australia (UWA). The tests were designed in such a way to complement and, hopefully, corroborate the findings of the numerical study, having adopted an anchor geometry and soil parameters different from those adopted in the FE analyses.

3.1 *Soil sample and experimental setup*

The prototype geometry of the model caisson (at 80 g) was characterized by external diameter $D = 3.2$ m, length over diameter ratio $L/D = 3$, and wall thickness $t = 40$ mm. The caisson lid was equipped with a differential pore pressure transducer, for the measurement of suction, and a valve operated during the tests by a remotely controlled motor.

The soil sample consisted of a homogeneous layer of soft clay. The undrained shear strength profile, derived by T-bar penetration tests performed prior to the caisson tests, was characterised by a gradient of 1.3 kPa/m. Core analysis of the clay sample, subsequent to testing, revealed an effective unit weight quite variable with depth, according to the expression $\gamma' = 3.935\ z^{0.1311}$ (with z in metres and γ' in kPa). Finally, the coefficient of horizontal consolidation, C_h, derived by in-fligth cone dissipation tests, varied in the range 27.3-33.2 m^2/yr for σ'_v varying in the range 33-50 kPa.

Each installation started with the caisson fully submerged and suspended above the mudline. An axial load cell, attached to the loading arm, measured the submerged weight of the caisson, that was zeroed before starting with the installation. Jacked installation was performed by monotonically penetrating the rigidly connected caisson and loading arm into the sample at a constant rate of 0.5 mm/s, with the drainage valve on the lid of the caisson open. After reaching the full penetration, the valve was closed to simulate a sealed lid and a setup period of 45 minutes (200 days prototype time) was allowed to let the excess p.w.p., induced during installation, dissipate. Over this period the caisson position was held constant. In test T02 only, the setup stage was omitted.

The first test (T01) was performed to assess the drained and undrained capacity of the soil foundation system. In this test only, the valve was kept open during the setup stage following the caisson installation. Subsequently, the caisson was pulled-out at a constant rate v of 0.001 mm/s, corresponding to a dimensionless velocity $V = vD/C_h = 0.06$ lower than 0.1, 0.1 being the threshold value, suggested by Chow et al.

(2020), for the drained response of kaolin clay. The uplift was stopped shortly after the peak was detected in the load-displacement plane, meaning that the drained capacity was fully mobilized. The caisson was then pushed back into the soil, the valve was closed and a new 45 minute setup stage was performed. Finally, the caisson was pulled out rapidly at a constant rate v of 2 mm/s, corresponding to $V = vD/C_h = 120$, high enough to expect an undrained response of the soil (Chow et al., 2020). The test was stopped shortly after the peak in the load-displacement plane was detected.

All remaining tests (T02-T05) were performed to assess the behaviour of the caisson under sustained loading. Therefore, after the caisson installation and setup stages, a prescribed vertical load was applied instantaneously at the top of the caisson by the actuator, operating under load control. The load was then held constant until the failure of the system eventually occurred. In the case of failure, the test was stopped when the caisson was fully extracted from the soil and its position was 10 mm above the seabed. The results of tests T02-T05 are discussed in the sequel.

3.2 *Results from physical modelling*

The unsealed and sealed pull-out tests (performed in T01) provided the following peak values of drained and undrained holding capacity: $V_u^{caiss} = 799$ kN and $V_u^{rev} = 1432$ kN, respectively.

As far as tests T02-T05 are concerned, a sustained load of 757 kN, 574 kN, 874 kN was applied in tests T02, T03 and T04, respectively, corresponding to a load level $V/V_u^{rev} = 0.56$ (T2), 0.43 (T3), 0.65 (T4). Test T05 differed from the others for the fact that two loading stages were performed: a load of 656 kN ($V/V_u^{rev} = 0.49$) was first applied and held for approximately 600 days; the load was then increased to 983 kN ($V/V_u^{rev} = 0.73$) and held constant until failure.

Tests T02, T04 and T05, ended with a failure of the soil-caisson system, while in test T03 the load was safely sustained for almost 11 years (prototype time) with negligible displacement of the caisson (0.0175m). The results of the sustained loading stage of tests T02, T04 and T05 are represented in terms of the measured load and caisson displacement over time in Figure 5, while the results of test T03 are here omitted. Negative values of load are used for uplift.

From Figure 5 it may be seen that, after an initial mobilization of the vertical displacement of the caisson as a result of application of the uplift load, an accumulation of the displacement is observed over time, increasing linearly at first and then at an increasing rate, with acceleration of the caisson upwards until failure and full extraction (vertical line in the displacement plot).

The type of failure observed in tests T02, T04, and T05 can be defined as a plug failure. Indeed, after the full extraction of the caisson, almost the same load value was measured by the load cell in all three tests: 364 kN (T02), 356 kN (T04), and 365 kN (T05). Such values match well the submerged weight of the soil plug, that can be estimated as $W'_{plug} = \sigma'_v(z = L)\, A'_i = 344$ kN, with A_i being the internal cross-sectional area of the caisson. Moreover, the 1g inspection at the end of the tests confirmed that the caisson was fully extracted carrying the intact plug within the skirts.

The results of the sustained loading tests are then compared to the predictive tool defined by Equation 1 in Figure 6, showing very satisfactory agreement. A logarithmic scale is adopted for the holding time axis to allow for better clarity of the representation. As far as the anchor points of the two curves defining the envelope are concerned, these are evaluated as: V_u^{rev} and V_u^{caiss} using test T01 results, and $V_u^{plug} = 0.5\, V_u^{caiss} + W'_{plug}$. In the previous calculation an embedded length of the caisson skirt equal to $L_{eff} = 9$ m ($L_{eff}/D = 2.81$), corresponding to the mean value of the effective embedded lengths in T02-T05, is considered.

From Figure 6 it is possible to observe that, for the case at hand, with $V_u^{plug} < V_u^{caiss}$, the prevailing failure mechanism, and the only one observed, is that of plug failure, being the one mobilized in a shorter time. By contrast, loads even slightly lower than V_u^{plug} are stable loads (orange lines in Fig. 6), that the caisson is able to sustain safely for a very long time.

4 Concluding remarks

In this paper the results of a numerical and physical investigation of the behaviour of suction caissons under sustained vertical loading have been presented. Based on an extensive set of fully hydro-mechanical coupled FE simulations, of which a limited part is presented here, equations of general validity have been obtained to describe the evolution of the holding capacity over time, the latter reducing as a consequence of the change of the soil drainage conditions under long-term loads. Such equations, based on the solutions of Terzaghi's one-dimensional consolidation, allow one to build an envelope describing the caisson behaviour at failure in load-time space.

The load-time failure envelope has been validated against the results of centrifuge tests, showing very satisfactory agreement. This encourages the use of the envelope as a predictive tool in pre-design computations. Indeed, the design envelope enables a designer to easily assess the holding time that can be relied upon for each load level expected during the service life of the offshore facility. Actually, the failure envelope can be used in a twofold way to ensure that an appropriate safety factor is maintained (i) on the load for the expected duration of the sustained loading event, and (ii) on the duration of the event for the expected sustained load level. In other words, the designer would have to compare the load with the holding capacity corresponding to the given duration of

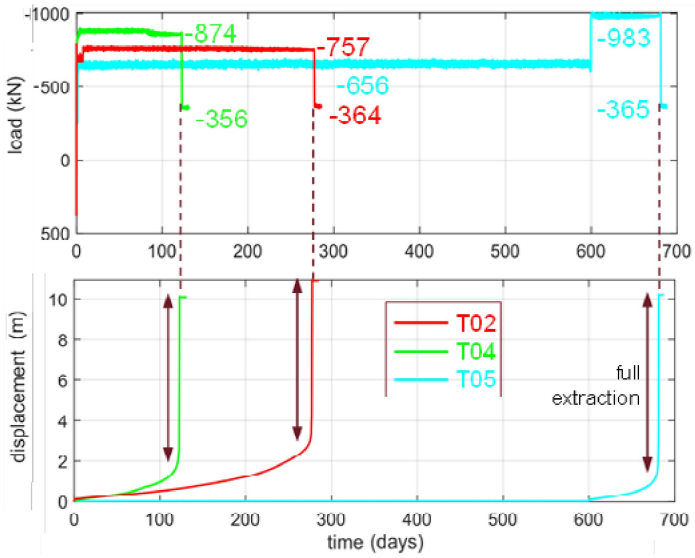

Figure 5. Load and caisson displacement measured during the sustained loading stage until failure (tests T02, T04, T05)

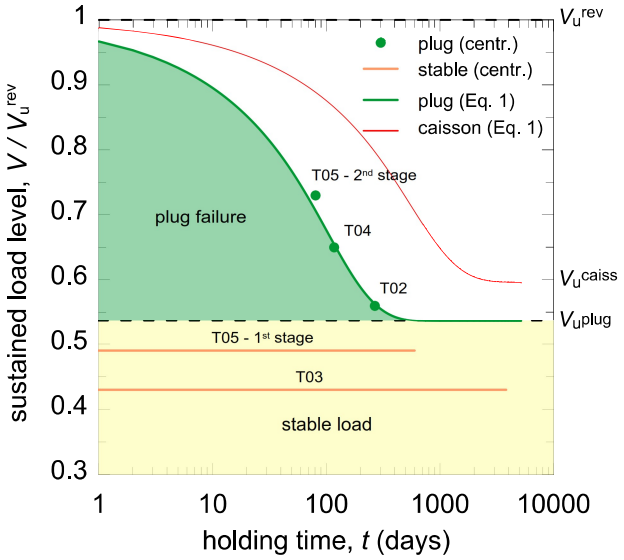

Figure 6. Results of tests T02-T05 (dots and orange lines) and analytical curves (Eq. 1)

the event in case (i), and the duration of the event with the limit holding time corresponding to the given load level in case (ii). The use of the proposed envelope would eventually lead to overcome common assumptions made in practice when approaching the design of anchors under sustained loading, such as very high values of the time safety factor (a value of 10 is suggested in Clukey et al., 2004), or, even more restrictively, total neglect of the potential contribution of passive suction in enhancing uplift resistance of suction caissons.

Acknowledgments

Centrifuge testing at the NGCF of UWA was made possible thanks to the approval of Prof. Conleth O'Loughlin. The Authors wish to acknowledge his support in the preparation of the testing program. A big hand behind the success of the tests was given by the chief centrifuge technician Mr Manuel Palacios whose help is gratefully acknowledged.

References

Al Khafaji Z, Audibert JM, Hossain MK, Templeton JS, Clukey EC and de Jong P. (2003). Suction caisson foundation design for vortex-induced vibration loading. OTC 15239, Proc. Offshore Tech. Conf., Houston, USA.

Andersen KH and Jostad HP. (2002). Shear strength along outside wall of suction anchors in clay after installation. In: Proceedings of the 12th International Offshore and Polar Engineering Conference, Kitakyushu, Japan.

Andersen KH and Jostad HP. (2004). Shear strength along inside of suction anchor skirt wall in clay. OTC 16844, Proc. Offshore Tech. Conf., Houston, USA.

Chen W and Randolph MF. (2007). Uplift capacity of suction caissons under sustained and cyclic loading in soft clay. Journal of Geotechnical and Geoenvironmental Engineering 133, 1352-1363.

Chen W, Zhou H and Randolph MF. (2009). Effect of installation methods on external shaft friction of caissons in soft clay. Journal of Geotechnical and Geoenvironmental Engineering 135 (5), 605–615.

Chow SH, O'Loughlin CD, Zhou Z, White DJ and Randolph MF. (2020). Penetrometer testing in a calcareous silt to explore changes in soil strength. Géotechnique 70, 12, 1160–1173.

Clukey EC and Phillips R. (2002). Centrifuge model tests to verify suction caisson capacities for taut and semi-taut legged mooring systems. Proceedings of Deep Offshore Technology Conference, New Orleans, USA.

Clukey EC, Templeton III JS, Randolph MF and Phillips R. (2004). Suction caisson response under sustained loop current loads. OTC 16843, Proc. Offshore Tech. Conf., Houston, USA.

Deng W and Carter J. (2002). A theoretical study of the vertical uplift capacity of suction caissons. International Journal of Offshore and Polar Engineering 12, 89–97.

Gourvenec S and Clukey E. (2018) Suction Caisson Anchors. In: Carlton J et al. (eds.). Encyclopedia of Maritime and Offshore Engineering, 2018. John Wiley & Sons Inc.

Jeanjean P, Znidarcic D, Phillips R, Ko H, Pfister S, Cinicioglu O and Schroeder K. (2006). Centrifuge testing on suction anchors: Double-wall, over-consolidated clay, and layered soil profile. OTC 18007, Proc. Offshore Tech. Conf., Houston, USA.

Mana SK, Gourvenec S, Randolph MF. (2014). Numerical modelling of seepage beneath skirted foundations subjected to vertical uplift. Computers and Geotechnics 55, 150–157.

Randolph MF and House AR. (2002). Analysis of suction caisson capacity in clay. OTC 14236, Proc. Offshore Tech. Conf., Houston, USA.

Randolph MF and Gourvenec S. (2011). Offshore geotechnical engineering. Spon Press, Abingdon, Oxon, 530pp.

Roscoe K and Burland J (1968). Engineering plasticity. Cambridge University Press, 1968, ch. On the Generalized Stress-Strain Behavior of Wet Clays, pp. 535–609.

Senders M and Randolph MF. (2009) CPT-based method for the installation of suction caissons in sand. Journal of Geotechnical and Geoenvironmental Engineering 135(1): 14-25